Master thesis : Experimental and numerical analysis of the aerodyanmics of the A&M Shell Eco-marathon vehicle prototype

Auteur : Calleja Vazquez, Juan Manuel

Promoteur(s) : Terrapon, Vincent

Faculté : Faculté des Sciences appliquées

Diplôme : Master en ingénieur civil en aérospatiale, à finalité spécialisée en "aerospace engineering"

Année académique : 2017-2018

URI/URL : http://hdl.handle.net/2268.2/4671

Experimental and numerical analysis of the aerodynamics of the *A&M* Shell Eco-marathon vehicle prototype

Juan Manuel Calleja Vázquez
Promoter: V.E. Terrapon

University of Liège: Faculty of Applied Sciences
Master in Aerospace Engineering
Academic year 2017-2018

The search for better performance is an actual challenge in the automotive industry. This is the reason why Shell proposes students from the entire globe to participate in its eco-marathon, a competition in which the maximum efficiency is searched. This thesis presents a numerical and experimental study of the *A&M* UrbanConcept vehicle: Electra. Wind tunnel conditions are simulated using RANS and URANS simulations in ANSYS FLUENT and compared to wind tunnel experimental data, allowing to validate numerical results. Once the numerical set-up is validated, a more in-depth study of Electra's aerodynamic properties is performed. In this study, track conditions are simulated and compared to wind tunnel conditions. This comparison allows to see the ground effect phenomenon and how it affects the aerodynamic properties of the car. Bearing in mind all simplifications made on the numerical model, aerodynamic corrections are applied to the obtained results. Then, a thorough discussion on surface imperfections and protuberances is made, being possible to estimate the drag value of the real car. Using this study, it is possible to modify the car geometry in order to improve its performance, achieving a drag decrease of 38% with respect to the original geometry. Finally, the aerodynamic effect that the introduction of a new platform chassis type could have on Electra's aerodynamics is tested and optimized.

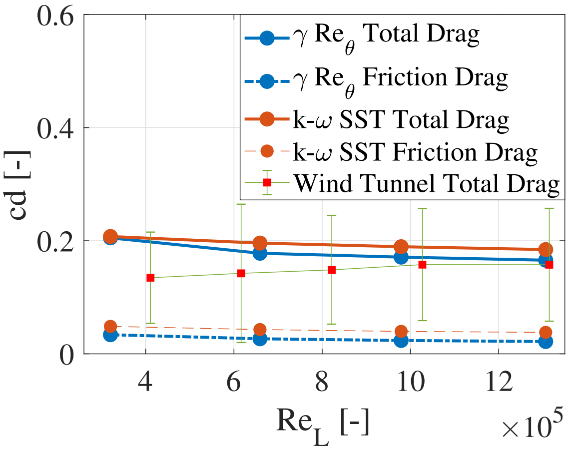

Figure 1: Drag coefficient at different length based Reynolds numbers obtained experimentally and with the low-Reynolds version of the $k - \omega$ SST model and the γRe_θ transition model, still road conditions and a $Re_L = 13 \times 10^5$.

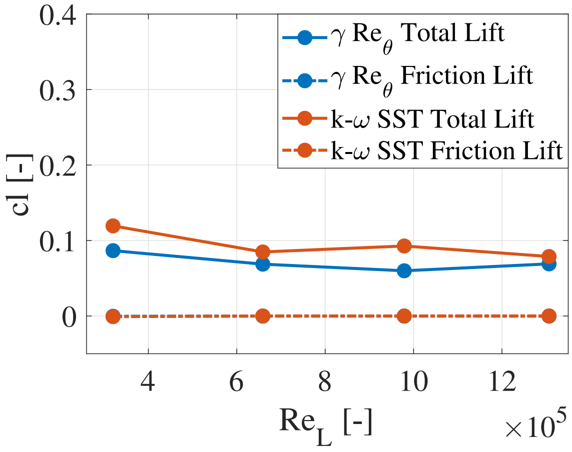

Figure 2: Lift coefficient at different length based Reynolds numbers obtained with the low-Reynolds version of the $k - \omega$ SST model and the γRe_θ transition model, still road conditions and a $Re_L = 13 \times 10^5$.

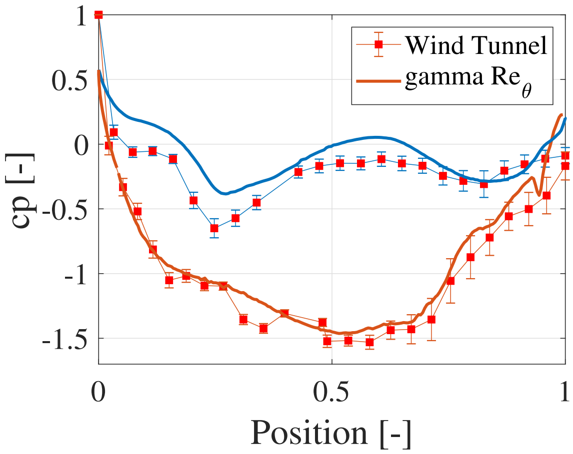

Figure 3: Experimental and numerical pressure coefficient distribution measured at Electra's symmetry plane at an angle of incidence of 30^o for a $Re_L = 8.2 \times 10^5$. Simulations performed with the γRe_θ model at still conditions. Lower surface in blue, upper surface in orange.

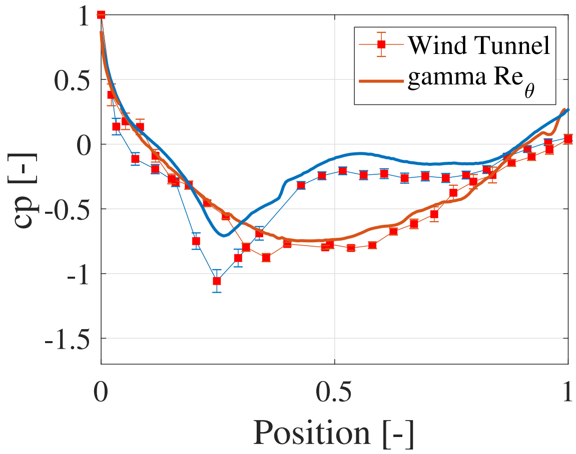

Figure 4: Experimental and numerical pressure coefficient distribution measured at Electra's symmetry plane at an angle of incidence of 15^o for a $Re_L = 8.2 \times 10^5$. Simulations performed with the γRe_θ model at still conditions. Lower surface in blue, upper surface in orange.

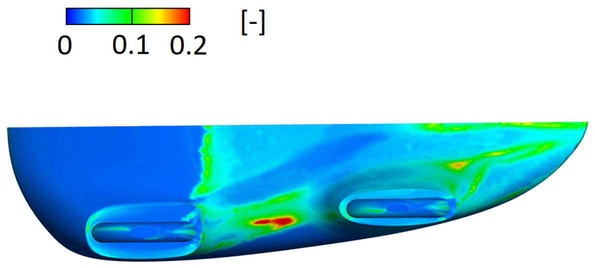

Figure 5: Intermittency contour plot at the car lower surface with moving road conditions. Simulation performed using the γRe_θ model at a $Re_L = 13 \times 10^5$.

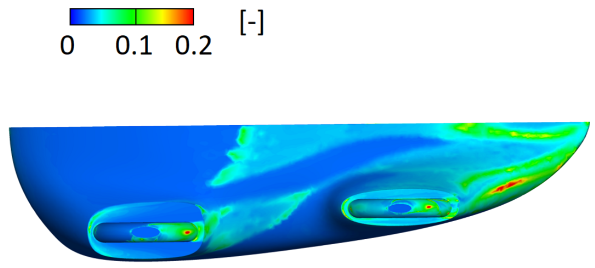

Figure 6: Intermittency contour plot at the car lower surface with still road conditions. Simulation performed using the γRe_θ model at a $Re_L = 13 \times 10^5$.

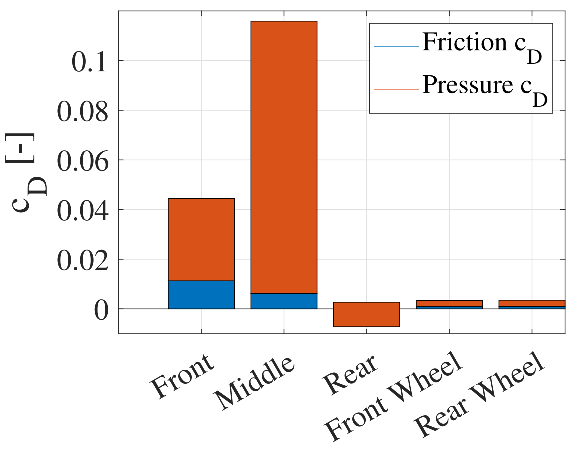

Figure 7: Histogram showing the distribution of pressure and friction drag on the different sections of Electra at still road conditions. Simulation performed using the γRe_θ model at a $Re_L = 13 \times 10^5$.

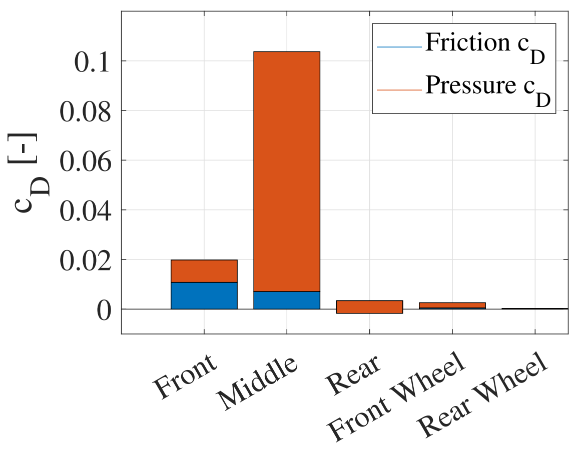

Figure 8: Histogram showing the distribution of pressure and friction drag on the different sections of Electra at moving road conditions. Simulation performed using the γRe_θ model at a $Re_L = 13 \times 10^5$.

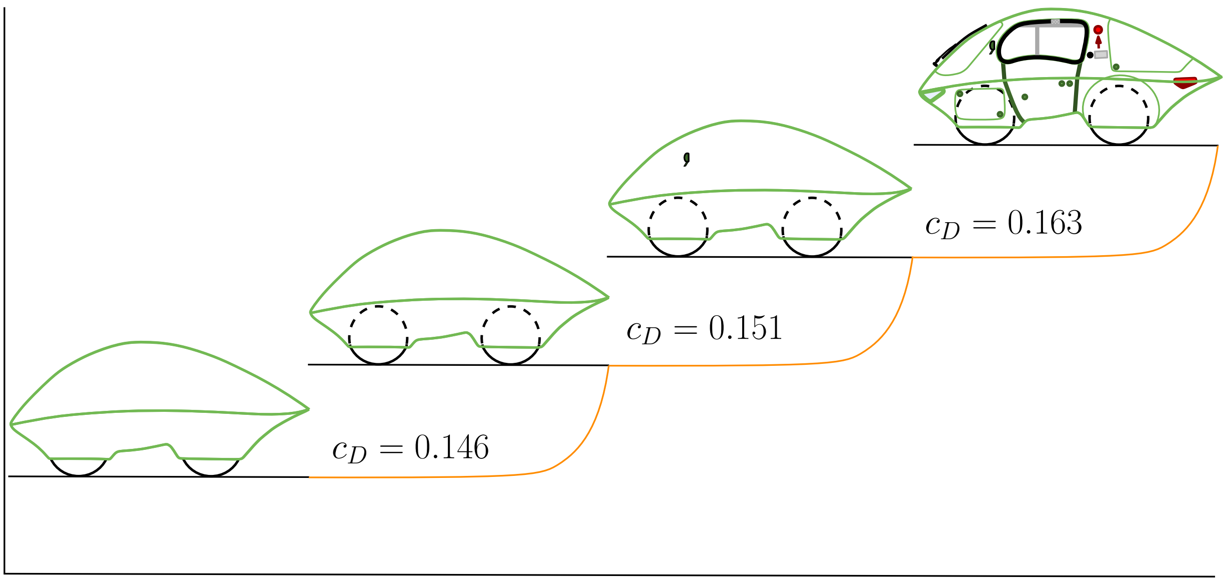

Figure 9: Electra drag coefficient and effect of the different simplifications. Simulation performed with the $\gamma Re\theta$ model at moving road conditions and a $Re_L = 13 \times 10^5$.

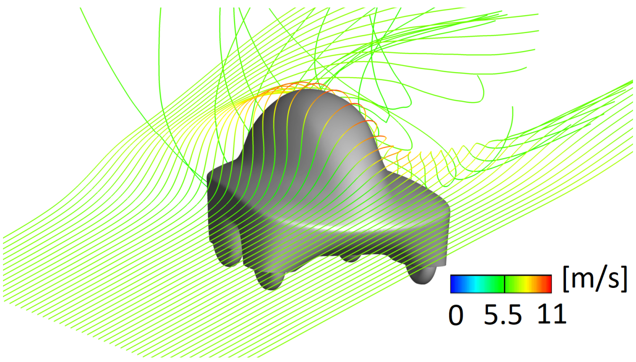

Figure 10: Flow streamlines over Electra upper section. Streamlines coloured by velocity magnitude. Moving road simulation performed with γRe_θ model at 30^o crosswind and a $Re_L = 8.2 \times 10^5$.

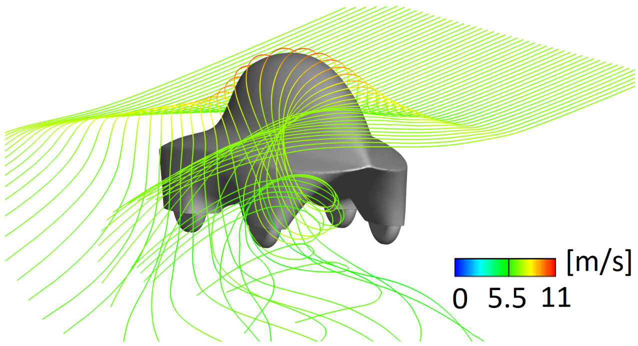

Figure 11: Flow streamlines over Electra upper section. Streamlines coloured by velocity magnitude. Moving road simulation performed with γRe_θ model at 30^o crosswind and a $Re_L = 8.2 \times 10^5$.

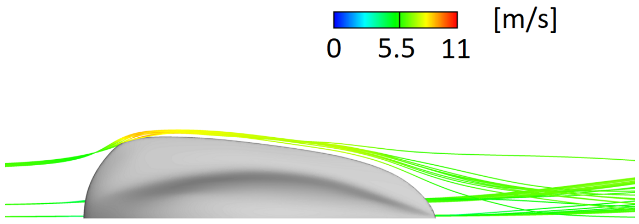

Figure 12: Flow streamlines over the third performance modification. Streamlines coloured by velocity magnitude. Simulation performed with moving road conditions using the γRe_θ model at a $Re_L = 13 \times 10^5$.

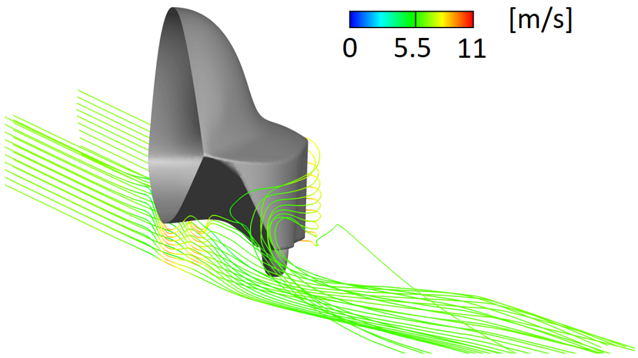

Figure 13: Flow streamlines over the third performance modification. Streamlines coloured by velocity magnitude. Simulation performed with moving road conditions using the γRe_θ model at a $Re_L = 13 \times 10^5$.

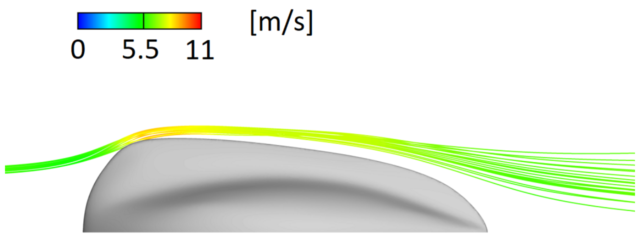

Figure 14: Turbulent kinetic energy contour plot at a $x = 0.15$ m $y - z$ plane. Simulation performed with second new concept modification at moving road conditions using the γRe_θ model at a $Re_L = 13 \times 10^5$.

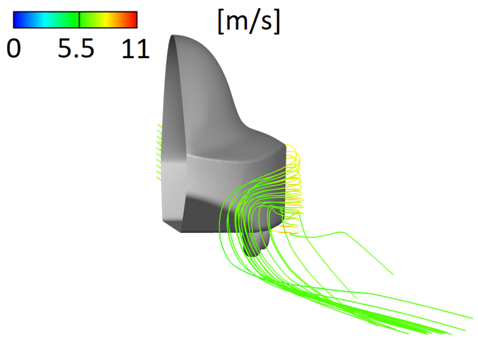

Figure 15: Turbulent kinetic energy contour plot at middle car plane. Simulation performed with second new concept modification at moving road conditions using the γRe_θ model at a $Re_L = 13 \times 10^5$.